Electric effects in the multicomponent ion-exchange kinetics

A.M. Dolgonosov *

*V.I. Vernadsky Institute of Geochemistry and Analytical Chemistry, Russian Academy of Sciences,
19 Kosygin Str, Moscow 117975, Russia*

Abstract

Kinetics of multicomponent ion exchange (MIE) is theoretically analyzed to reveal the occurrence of macroscopic electric fields. An experimental technique to detect these fields is proposed. Self-oscillations in MIE systems are described. Relations between the amount of microcomponent introduced into a MIE system and its reply electric signal are determined.

Keywords: Kinetics; Multicomponent ion exchange; Macroscopic electric field; Self-oscillations

1. Introduction

In [1,2], a macroscopic model for the multicomponent ion-exchange (MIE) kinetics was described. The model is based on the hypothesis that electric fields accompanying the kinetic process reveal, in essence, a macroscopic behaviour.

According to the electroneutrality condition, in the ion-exchange intraparticle diffusion the total charge of counterions under the thermodynamic equilibrium must be equal to the total charge of functional groups of anion exchanger:

$$\sum z_i a_i \approx \sum z_i a_{0i} = a_0 = \text{const} \qquad (1)$$

where z_i is the ion charge, a_{0i} is the equilibrium ion concentration in the exchanger (mmol/cm^3), and a_0 is the equivalent concentration of functional groups (meq/cm^3). The approximate equality in Eq. 1 fulfils with a high accuracy because the relaxation to a local equilibrium requires much less time than that to the total thermodynamic equilibrium in the ion-exchange system.

It is the incomplete compensation of the charges that gives rise to radial dipole moments in a grain of the ion exchanger that generates a spherically symmetric electric field tending to countervail these dipoles. This is the main feature of the macromodel proposed in [1,2] unlike the local model of [3] in which the electric field emerged is considered at the microscale. The use of the local model leads to complex mathematical problems related to the integration of second-order nonlinear partial differential equations. Our hypothesis concerning the macroscopic behaviour of the electric field in an ion-exchange grain makes it possible to simplify its mathematical formulation. This paper discusses the basic question: *does the macroscopic electric field really affect the ion-exchange kinetics?*

In the macromodel, the ion-exchange kinetic

* Corresponding author.

equation accounting for the electric potential φ can be written as:

$$\frac{da_i}{dt} = \frac{12\alpha D_i}{d^2}\left\{ a_{0i} - a_i\left[1 - \frac{\alpha_1 F z_i}{RT}(\varphi_0 - \varphi)\right]\right\}$$

(2)

where α, α_1 = const, d is the exchanger grain diameter, D_i is the ion diffusivity, F is the Faraday constant, T is the temperature, φ_0 is the equilibrium potential. The expression $\alpha_1(\varphi_0 - \varphi)$ can be derived from the condition

$$\sum z_i \frac{da_i}{dt} = 0$$

(3)

which is satisfied with a high accuracy as well as Eq. 1, that implies

$$\alpha_1(\varphi_0 - \varphi) = \frac{-RT}{F} \cdot \frac{\sum D_j z_j (a_{0j} - a_j)}{\sum D_j z_j^2 a_j}$$

(4)

Substitution of Eq. 4 in Eq. 2 yields:

$$\frac{da_i}{dt} = \frac{12\alpha D_i}{d^2} \times$$

$$\left\{ a_{0i} - a_i \qquad \frac{z_i \sum D_j z_j (a_{0j} - a_j)}{\sum D_j z_j^2 a_j} \right.$$

(5)

Assuming $\varphi_0 - \varphi = 0$ in Eq. 2, we come to the familiar kinetic approximation formulated by Glueckauf [4]. The basic limitation of the glueckauf approach is that the parameters D_i are time-dependent, whereas in the macromodel approach the diffusivities D_i are constant, but the potential φ is time-dependent.

Let us consider the occurrence of a maximum on the kinetics curves: (a) the maximum arises on the kinetic curve for the most mobile of the competing ions; this was also concluded in [3]; (b) the desorbed component diffusivity is to be greater than the diffusivity for at least one of the competing components; (c) the larger the difference in diffusivities of the competing components as well in diffusivities of the desorbed component and the slowest of the competing ones, the larger the effect; (d) the smaller the equilibrium concentration of the most mobile component in the ion exchanger, the larger the effect.

Calculations by Eqs. 4 and 5 of the time derivative of the potential versus time yield the Gaussian curve of which maximum is close enough to the kinetic curve maximum. This implies that in the neighbourhood of the kinetic curve maximum $da_x/dt \approx 0$ and Eq. 4 can be written as:

$$\alpha_1(\varphi_0 - \varphi) \approx \frac{-RT}{F} \cdot \frac{a_{0x} - a_x}{z_x a_x} \equiv \frac{RT}{F z_x} \cdot \Delta_x$$

(6)

Thus, we can conclude that the relative overshoot (Δ_x) of the peak maximum over the equilibrium ion content (x) is the main reason why the electric potential (φ) deviates from the equilibrium value (φ_0).

The second conclusion from the theory is that the electric field magnitude significantly decreases as co-ions (e.g., anions in the cation-exchange process) penetrate into the ion exchanger. This is due to an arbitrary distribution of the co-ions within the electric field organized by the counterions. Indeed, the Donnan effect, i.e. the boundary electrostatic barrier of the same polarity as the co-ions, prevents their penetration inward the ion exchanger. A combination of the macroscopic electric field arising in the ion-exchange process and the Donnan electrostatic potential can lead to self-oscillations in the system. This possibility was verified in experiment as described below.

2. Experimental

The experimental device is shown in Fig. 1. It consists of an ion-exchange membrane (1) that separates three hydraulically nonconnected cells: a working cell (2), a supporting cell (3) and a pure cell (4). The membrane potentials were measured by a grid electrode (5) and an orificed electrode (6). These electrodes were connected by a series condenser (7) (15 μF) to the center (1 MΩ) of a double-coordinate voltmeter-recorder (8) (ENDIM 622.02, Germany). The cation-exchange membrane (MK-40, Russia) had a round shape 20 mm in diameter and 1 mm in thickness. The electrodes were prepared of
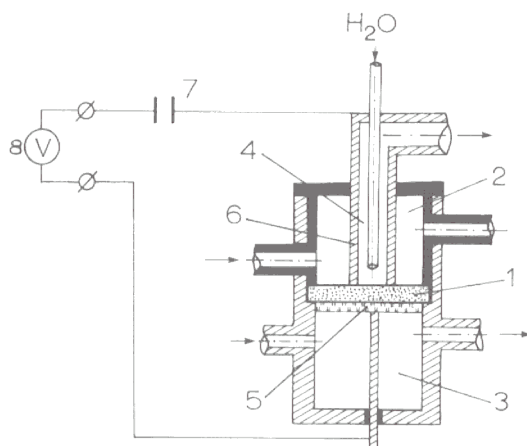
Fig. 1. Schematic of three-component ion-exchange system and electric circuit for measurement: (1) ion-exchange membrane; (2) working cell; (3) supporting cell; (4) pure cell; (5) grid electrode; (6) orificed electrode; (7) condenser; (8) two-coordinate voltmeter-recorder.
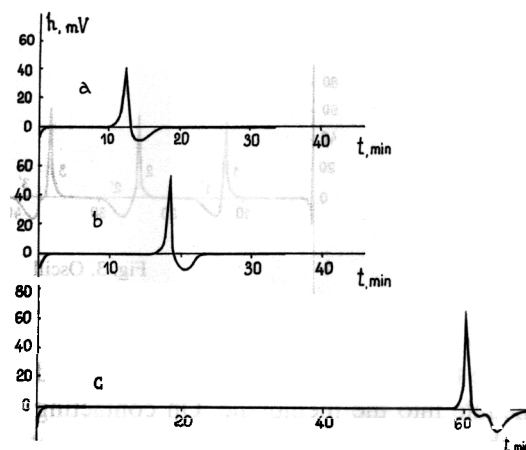

Fig. 2. Oscillograms for the three-component ion-exchange system (hydrogen, sodium and potassium ions). Conditions as described in Experimental. Potassium concentration (ppm): (a) 10; (b) 5; (c) 1.

stainless steel. The pure cell contained doubly distilled water whereas the supporting and working cells contained 0.75 mM H_2SO_4 and 25 mM Na_2SO_4, respectively. The flow-rate of each solution was 0.5–1.0 cm^3/min (the so-called 'basic regime'). Before measurements, the system was conditioned at least for one hour. Then, the flow of sodium sulfate solution was switched off and the working cell was flushed out with water. At the beginning of each experiment, the potassium sulfate solution 3 cm^3 by volume was injected in the working cell, its concentration varying from 15 μM to 1 mM. After 2-minute contact of the membrane with the potassium sulfate solution, the latter was displaced by the sodium sulfate solution passed through the working cell like in the basic regime. All the chemicals used were of the analytical-reagent grade.

3. Results and discussion

Fig. 2 demonstrates the time derivative of the membrane potential as a function of time (this plot we named the 'oscillogram' similar to curves displayed on the oscillographic screen). As is seen from Fig. 2, the initial oscillogram recorded before the experiment starts is a horizontal line with y = cont. At the onset of the experiment,

the oscillogram looks like an extended horizontal line followed by a narrow peak 60–100 mV in amplitude and then by a trough of the opposite polarity, approximately equal to the peak by its area. The peak waiting time correlates with the amount of injected potassium so that the higher the concentration, the smaller the peak waiting time. For example, 10 ppm K^+ yields the peak waiting time 12–14 min, 5 ppm K^+ – 16–18 min, 1–2 ppm K^+ – 61–64 min. When the injected potassium amount exceeds some threshold (about 0.5 mM), on the oscillogram there appear several peaks at equal intervals (about 10 min) beyond the corresponding trough (Fig. 3).

From the above theoretical approach, the behaviour of the MIE system can be explained as follows. The basic state of the system corresponds to the steady separation of the zones of sodium and hydrogen cations within the membrane of the potential φ_0 (here we mean not the total potential but its kinetic component involved in Eqs. 2–6; the other component on the membrane surface is the Donnan potential). The potential φ_0 of the orificed electrode has a positive value because it equalizes the velocities of highly mobile hydrogen ions and slow sodium ions. We chose such experimental conditions that the potential φ_0 did not completely com-
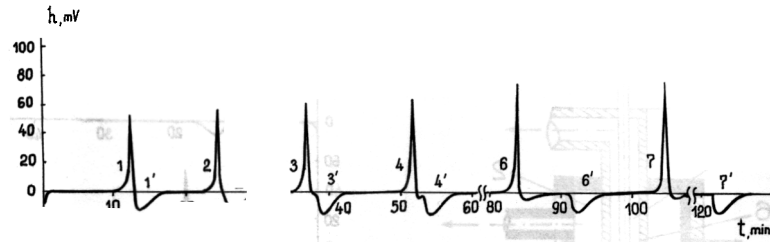
Fig. 3. Oscillogram for 0.5 mM potassium.

pensate the Donnan potential and anions did not penetrate into the membrane. On contacting the membrane with potassium ions, their front is, at first, far from the boundary of macrocomponent zones. Therefore, the boundary is not shifted and the potential of the system is maintained. When potassium ions (less mobile in the cation exchanger than sodium ions) reach the boundary, hydrogen ions become more retarded that results in increasing the positive potential of the orificed electrode. Under the experimental conditions chosen, this increase completely compensates the Donnan potential so that sulfate ions penetrate from the working cell into the membrane sharply changing the pattern of ionic currents and thus fast lowering the membrane potential to very low values. This step of the process is displayed as the peak on the oscillogram. At the same moment, the Donnan potential at the side of working cell is restored and, consequently, the flux of anions into the membrane is terminated and the anions now release with hydrogen ions into the pure cell. This step – restoring the membrane potential – is depicted as the trough on the oscillogram.

It is apparent that the amount of the potassium injected at the onset of the experiment affects the parameters of the potassium front in the membrane. The maximum gradient of microcomponent (potassium) concentration in the ion exchanger can be determined by he expression:

$$(\text{grad}\, a_x)_{\max} = \frac{c_0\sqrt{\Gamma_x}}{\lambda} \le \frac{\sqrt{a_0 c_0 K_{x0}}}{\lambda} \qquad (7)$$

where c_0 is the macrocomponent (here, sodium) concentration, Γ_x is the microcomponent (potas-

sium) distribution coefficient, K_{x0} is the potassium selectivity constant, and λ is the distance between the membrane surface (from the side of working cell) and the boundary of macrocomponent zones. Eq. (7) implies that the front speed falls to a minimum and its slope rises to a maximum as the microcomponent concentration decreases to the limit when the distribution coefficient takes its maximum value $a_0 K_{x0}/c_0$. Above this limit, the lower microcomponent concentrations correspond to the larger peak waiting times and, what is quite not obvious, to the stronger compensation of the Donnan effect. The latter is accompanied by more intensive penetration of the anions into the membrane and consequently yields the higher peak and the longer peak–trough distance.

Fig. 3 demonstrates the self-oscillations in the MIE system with the flat immobile boundary between the macrocomponent zones. In this system it is possible to form a periodic, two-wave pattern of the microcomponent zone, parallel to the boundary (if the microcomponent is in a sufficient amount). Indeed, when the potassium front reaches the boundary between the sodium and hydrogen ion zones, the sodium is quickly displace from the contact zone into the working cell (the above property (a) of the ion-exchange kinetics). Removing the sodium ions from the boundary decreases the displacement velocity because of breaking the conditions necessary for this kinetic effect. As mentioned above, the penetration of co-ions into the membrane also breaks this effect. The displaced sodium front is finally stopped within the potassium zone and thereby divides it into two parts. On restoring the ba-

sic potential, the former higher velocity of alkali cations is also restored. The potassium front again reaches the boundary and the process repeats. the oscillations terminate only when the potassium amount in its last zone is not enough for creating the potential which can compensate the Donnan barrier.

This explanation is confirmed, in particular, by the fact that the distance between a trough and the next peak remains constant, despite growing the distance between peaks (as a result of decreasing the potassium amount in every new front). The fact that the amount of a microcomponent and its ion-exchange properties affect the characteristics of the described effect is of interest in chemical analysis.

Acknowledgements

References

[1] A.M. Dolgonosov, R.Kh. Khamizov, A.N. Krachak, A.G. Prudkovskii, React. Funct. Polym. 28 (1995) 13.
[2] A.M. Dolgonosov, R.Kh. Khamizov, A.N. Krachak, A.G. Prudkovskii, Dokl. Akad. Nauk 342 (1995) 53.
[3] Y.-L. Hwang, F.G. Helfferich, React. Polym. 5 (1987) 237.
[4] E. Glueckauf, Trans. Faraday Soc. 51 (1955) 34.